Journal of Hazardous Materials 321 (2017) 307–315

Contents lists available at ScienceDirect

Journal of Hazardous Materials

journal homepage: www.elsevier.com/locate/jhazmat

A combined microbial desalination cell and electrodialysis system for copper-containing wastewater treatment and high-salinity-water desalination

Yue Dong [a], Junfeng Liu [a], Mingrui Sui [a], Youpeng Qu [b,*], John J. Ambuchi [a], Haiman Wang [a], Yujie Feng [a,*]

[a] State Key Laboratory of Urban Water Resource and Environment, Harbin Institute of Technology, No 73 Huanghe Road, Nangang District, Harbin 150090, China

[b] School of Life Science and Technology, Harbin Institute of Technology, No. 2 Yikuang Street, Nangang District, Harbin 150080, China

HIGHLIGHTS

- Alkalinity produced in MDCs was used for treatment of copper-containing wastewater.
- There was nearly complete removal of copper after treatment of precipitation.
- An MDC-powered electrodialysis system was presented as deep desalination step.
- Energy balance was built for performance evaluation of the combined MDC-ED system.
- The real-world application prospect of the system was also analyzed.

ARTICLE INFO

Article history:
Received 25 June 2016
Received in revised form 6 August 2016
Accepted 11 August 2016
Available online 12 August 2016

Keywords:
Microbial desalination cell
Alkalinity production
Copper-containing wastewater treatment
High-salinity-water desalination

ABSTRACT

A new concept for heavy metal removal by forming hydroxide precipitation using alkalinity produced by microbial desalination cell (MDC) was proposed. Four five-chamber MDCs were hydraulically connected to concurrently produce alkalinity to treat synthetic copper-containing wastewater and salt removal. There was nearly complete removal of copper, with a maximum removal rate of 5.07 kg/(m^3 d) under the initial copper concentration of 5000 mg/L (final pH of 7). The final copper concentration met the emission standard for electroplating of China (0.5 mg/L, GB 21900-2008). XRD analysis indicated copper was precipitated as $Cu_2Cl(OH)_3$. The best performance of MDCs in terms of average power density, salt removal and COD removal rate achieved in stage 3 were 737.3 ± 201.1 mW/m^2, 53.6 ± 0.8 kg/(m^3 d), and 1.84 ± 0.05 kgCOD/(m^3 d) respectively. For purposes of water recovery, an electrodialysis (ED) system was presented based on in-situ utilization of generated electricity by MDCs as post-desalination treatment for salt effluent after sedimentation. The maximum discharging voltage of 12.75 ± 1.26 V at switching time (T_s) of 15 min using a capacitor-based circuit produced a maximum desalination efficiency of 30.4 ± 2.6%. These results indicated that this combined system holds great promise for real-world treatment of copper-containing wastewater and deep desalination of high-salinity-water.

1. Introduction

Water pollution is a serious environmental issue, which has posed a potential threat to human health and socio-economic development [1]. Insufficient treatment of domestic wastewater and heavy metal wastewaters presents to be one of the major challenges, which would exacerbate shortage of fresh water [2,3]. As reported, 1.2 billion people are suffering from shortage of fresh water and another 500 million people are approaching this situation [4]. Efficient treatment of polluted water for reclamation especially for those heavy metal wastewaters and extending the supply of fresh water might offer the option of alleviating shortage of fresh water.

* Corresponding authors.
E-mail address: yujief@hit.edu.cn (Y. Feng).

http://dx.doi.org/10.1016/j.jhazmat.2016.08.034
0304-3894/

In terms of domestic wastewater treatment, microbial electrochemical process has been proved to be effective to accelerate the degradation of organic matter in domestic wastewater [5]. The tough part was the purification of heavy metal wastewaters. Many approaches have been used to treat heavy metal wastewaters, such as chemical precipitation, ion-exchange, adsorption, membrane filtration, and electrodialysis [6,7]. Those commonly used technologies are efficient in removing metals, but require huge extra energy input such as electricity, high temperature and high pressure. Previous laboratory researches involving removal of heavy metal from wastewater have typically focused on the removal efficiency of targeted heavy metal, with little consideration given to the consumption of energy needed for the treatment process. For real-world applications, these input would likely multiplied as the size of the system increases due to other losses in systems scaling up, which set up a barrier to sustainable industrial application. Compared with the energy-intensive technologies, hydroxide precipitation with negligible energy input using sodium hydroxide (NaOH) and lime (CaO) may be the most common and effective method [8]. However, present preparation technologies of these precipitating agents such as causticizing and electrolysis method consume considerable heat or electricity [9,10]. It is also believed that secondary pollution exists in the manufacturing process of those chemicals [11]. Therefore, it would be viable if an energy-saving or even energy-generating technology offers the option of alkalinity production.

In respect of extending the supply of fresh water, high-salinity-water desalination has gained its popularity, especially in arid regions [12]. Recently, microbial desalination cell (MDC) has been developed as a promising technology due to the desalination and simultaneous electricity generation functionality [13,14]. A simple MDC contains three chambers, with a middle desalination chamber separated from anode chamber by an anion exchange membrane (AEM), and a cathode chamber by a cation exchange membrane [15]. The performance of desalination can be magnified by using more than one membrane pair between electrodes [16]. However, pH imbalance in both anode and cathode chambers resulting from hindered ion migration due to use of membrane, presents a big obstacle for extent of desalination and electricity production. This situation could be more serious in a stacked MDC system, where a significant salinity gradient across membranes results in junction potential enhancing the voltage output of whole system [17]. Once voltage output increases, there is more protons release in anolyte and more hydroxyl anions release into the catholyte to balance charges. But it is noteworthy to understand that one unit decrease in pH would significantly inhibit bacterial activity and lead to a complete failure of anode (pH < 6) [18]. Nevertheless, the change of pH on cathode performance appears to be relatively minor compared to its effect on anode (potential loss of 0.095 V per unit of pH) [19]. It is therefore possible to maximize the alkalinity production while having no significant negative impact on MDC performance.

A combined system for simultaneous treatment of domestic wastewater and heavy metal wastewater, as well as high-salinity-water desalination was established in this study. Four five-chamber MDCs with a desalination chamber and two concentrate chambers were hydraulically connected for desalination and alkalinity generation, and heavy metal copper was chosen as the targeted pollutant. In this study, we investigated the system performance in terms of desalination, power generation and copper removal efficiency. For purposes of water recovery, an electrodialysis (ED) system was presented as post-desalination treatment for salt effluent after sedimentation. The feasibility of in-situ of the generated electricity by MDCs for ED system was investigated, and the desalination performance was evaluated comparing to that of using DC power supply.

2. Materials and methods

2.1. Reactor construction

Design of the MDC was based on a previous described five-chamber MDC (one anode chamber, two desalination chambers, one concentrated chamber, and one cathode chamber). The five chambers were made of Plexiglas, and possessed the same cross-section dimension of 150 cm^2 (15 cm long, 10 cm high). The thickness for anode chamber was 50 mm, 5 mm for cathode chamber, and 3 mm for desalination and concentrated chamber. The anode chamber, concentrate chamber, desalination chamber, and cathode chamber were separated by alternating anion-exchange membranes (AEMs) and cation exchange membranes (CEMs). One row of anode was constituted by parallel placed four carbon brushes, which were externally woven onto a titanium wire (3 cm diameter by 10 cm length). Cathode was made by "rolling-press" method using activated carbon and PTFE [20]. All the chambers were clamped together by stainless steel fasteners and silica gel plates were inserted between membranes and chambers to prevent water leakage (Fig. 1).

The ED stack comprised three repeating cells, each consisted of a cation exchange membrane and an anion exchange membrane (Fig. 1). Theses membranes were separated by silicone gaskets forming flow channels for alternating concentrate and dilute. The area of the membrane was 54 cm^2. A squared electrode was placed on both sides of the membrane stack. The stainless steel sheet (6×9 cm) was used as electrodes. Thickness of the flow channel was 3 mm, by inserting a woven PET fabric spacer into the compartment of membranes.

2.2. Operating conditions

The MDCs were inoculated with domestic wastewater (20%, v/v) and operated in fed-batch mode. The medium contained glucose (1 g/L) in a 50 mM phosphate buffer solution (PBS) containing trace minerals and vitamins as previously described [21]. The desalination chambers were filled with 35 g/L NaCl in distilled water, while the concentrate chambers were filled with tap water. The cathode chambers were filled with 50 mM PBS buffer. Each MDC was operated with fixed hydraulic retention time (HRT) of 24 h during the start-up period, with stepwise reduced external resistance from 500 Ω to 100 Ω and finally to 10 Ω where it was maintained.

After a stable voltage output was observed, a series of hydraulically connected MDCs were assembled and operated in continuous flow mode. The medium was in turn flowed from MDC-1 to MDC-4. Salt solution (35 g/L) was pumped from MDC-1 to MDC-4 in turn through two separate flow line. Tap water was first pumped into the concentrate chamber of MDC-1, and then to MDCs two through four. The concentrate effluent was used as influent for the cathode chamber of MDC-1, and from there it flowed on to the other three reactors. The MDC performance under various operating conditions was evaluated. According to the operating conditions, the entire experimental period was divided into 4 stages, and the detailed operating parameters are summarized in Table 1.

Heavy metal precipitation test was conducted in the settlement tank by mixing catholyte effluent with synthetic copper-containing wastewater ($CuCl_2$) together with various initial copper concentrations (800, 1000, 1500, 5000 mg/L), with the HRT for the sedimentation tank setting at 5 h. The initial pH was adjusted to 3 using 1 M HCl based on the fact that almost all real heavy metal wastewaters presented to be strongly acidic [22]. An ED system was presented for further salinity removal of the effluent from the settlement tank. The concentrate solution was introduced from the anode side and flowed serially through every concentrate cell. Similarly, the dilute solution flowed through each of dilute cells. The

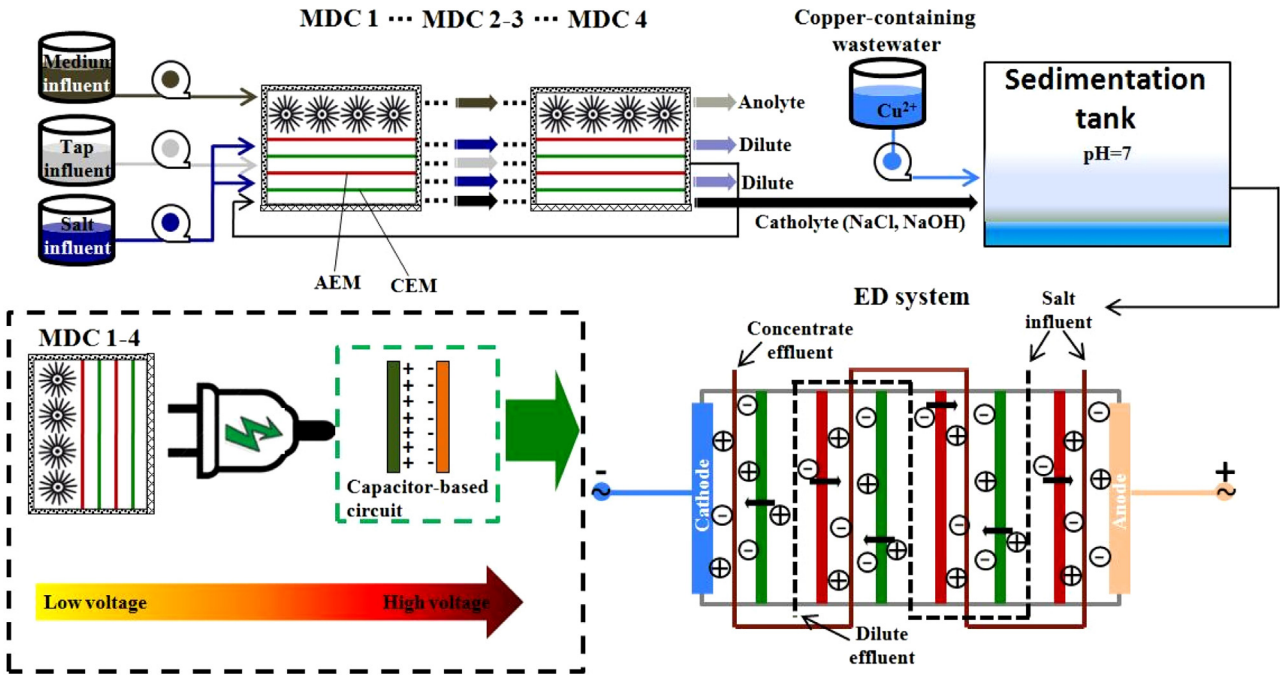

Fig. 1. Schematic of the experimental setup.

Table 1
Operation parameters and performances of the MDCs.

Stage	HRT (h)			Salt removal (%)	COD removal (%)	pH	
	Anode	Desalination chamber	Concentrate chamber			Anolyte	Catholyte
1	24	24	12	50.9 ± 3.5	86.8 ± 3.5	4.43 ± 0.17	10.72 ± 0.03
2	12	24	12	55.9 ± 2.9	84.8 ± 3.2	6.18 ± 0.16	10.65 ± 0.08
3	12	24	6	76.5 ± 1.2	92.2 ± 2.6	5.95 ± 0.08	10.56 ± 0.07
4	12	24	3	68.8 ± 1.6	73.4 ± 2.1	5.95 ± 0.02	10.55 ± 0.04

Note: each HRT was set based on the total volume of the 4 MDCs.

flow rates were equal in the concentrate and dilute channel and were set to match the effluent flow rate of the settlement tank. A boost circuit was used to harvest the electricity generated by MDCs (The HRTs for each chamber were identical to those in stage 3) to power the ED system (Fig. S1). This ED desalination experiment was also performed under constant voltage condition using a DC power supply (10, 11, 12, 13, 14 V). Salinities of the dilute and concentration were characterized in terms of conductivity.

2.3. Analyses and calculation

MDC voltages (U) were recorded every 30 min across a fixed external resistance of 10 Ω using a data acquisition system (Posi-813, ICP DAS Co., Ltd). Current was calculated using Ohm's law ($I = U/R$), with power calculated as $P = IU$. A reference electrode (Ag/AgCl; +200 mV vs standard hydrogen electrode, SHE) was inserted into the anode chamber to determine the anode and cathode potentials. Polarization and power curves were obtained by changing the external resistance from open circuit to 2.7 Ω. COD was measured using standard methods, and sample for COD measurement was firstly filtered through a 0.45 μm pore diameter syringe filters. The pH was measured using a pH meter and probe (Pb-10, Sartorius Ltd, Germany). The salt solution was analyzed in term of conductivity using a conductivity meter and probe (DDS-307, SPSIC-Rex Instrument Factory, China). The effects of OH^- on conductivity were neglected due to its low concentration (0.0001 M at pH = 10). Further, COD removal rate (kgCOD/(m^3 day)) was calculated based on COD removal per day and the volume of the medium. The NaCl removal rate (kg/(m^3 day)) was calculated by the NaCl removal per day based on reactor volume of the medium. The copper concentration in the form of Cu^{2+} in the samples was determined with an inductively coupled plasma-optical emission spectrometer (ICP-OES; Vista-MPX, Varian, Inc.). The X-ray diffraction patterns (XRD) were recorded on an X-ray diffractometer (D8 Advance, Bruker, Germany). The average discharging power of the capacitor-based circuit was calculated as previous described [23].

3. Results and discussion

3.1. Electricity generation and COD removal

To evaluate the electricity producing ability of the four MDCs at various HRTs, the polarization curves were measured at the end of each run to determine the maximum power densities (Fig. 2). The first MDC (MDC-1) of the four MDCs operated in series exhibited the best performance in terms of electricity generation in each stage, compared to the three downstream MDCs. The average maximum power densities of four MDCs during 4 operating stages decreased from 843.1 ± 49.3 (MDC-1) to 257.9 ± 167.4 mW/m^2 (MDC-4) along the direction of fluid flow. The decrease in power was likely due to a combination of factors that included the reduced COD concentrations in anode chamber, an anabatic pH imbalance between

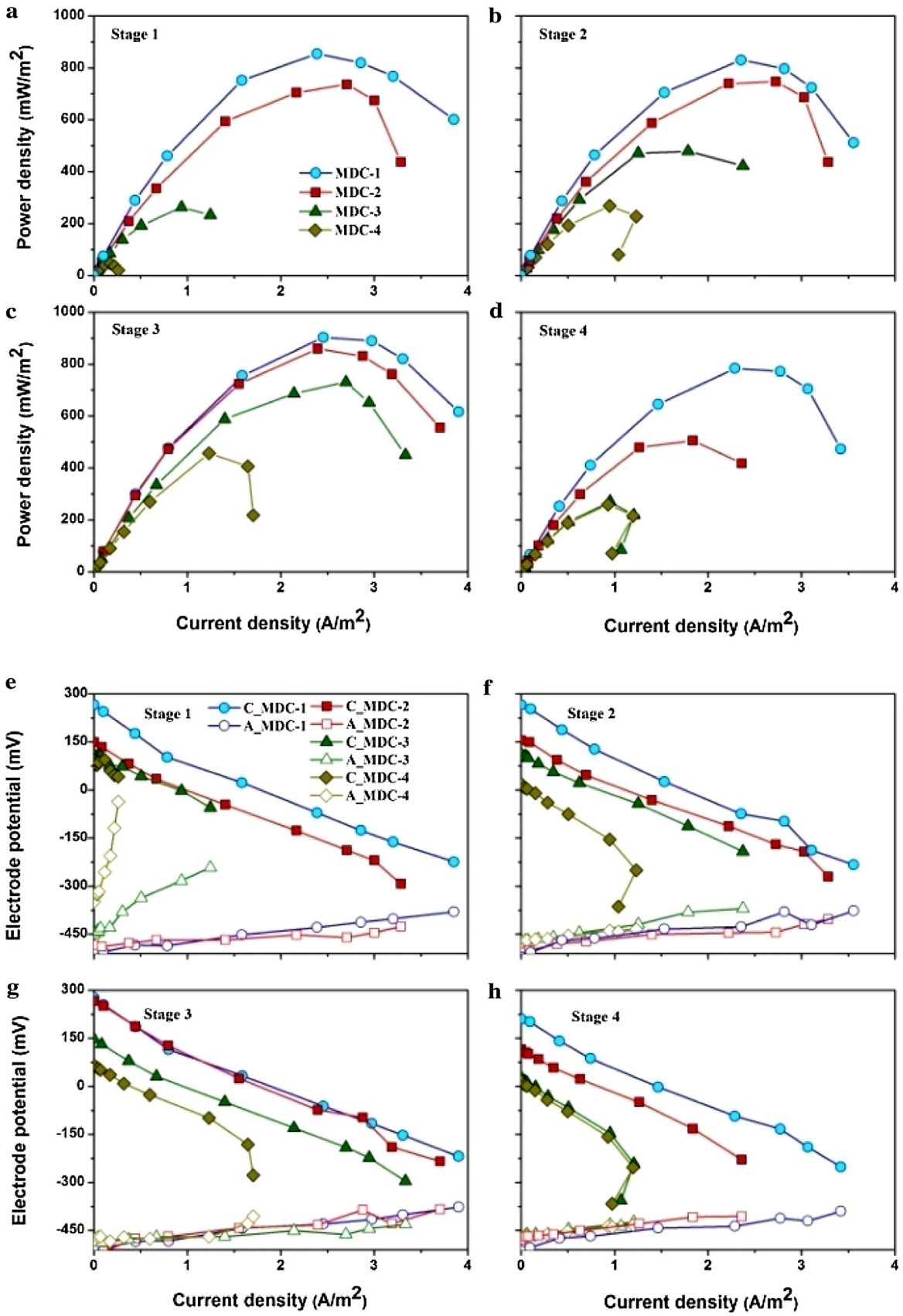

Fig. 2. Power densities (a–d) and change of the cathode and anode potentials (e–h) of the four MDCs in four stages.

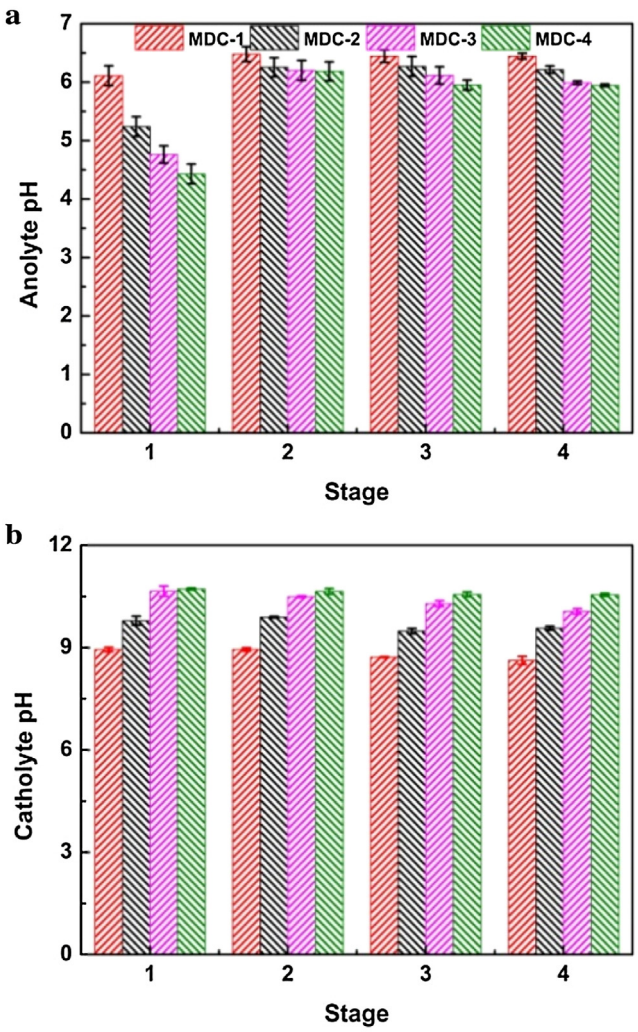

Fig. 3. The anolyte and catholyte pHs variation of the MDCs in four stages.

the anode and cathode chambers, and increased internal resistance in the middle desalination stack. Compared with the internal resistance of MDC-1 ($9.9 \pm 3.2\ \Omega$), the internal resistance of MDC-4 increased nearly 4 times ($39.3 \pm 13.3\ \Omega$), which to some extent, explained the sharp decline of power generation in downstream MDCs. The salinity gradient power resulting from reversible mixing of salt solutions with high and low concentrations also contributed to the difference of power densities. HRT is one of the important parameters for desalination process, as it significantly affected the electricity generation of this system. In each stage, the mean maximum power densities of the four reactors also differed at various HRTs. The average maximum power density of the four MDCs in stage 3 ($737.3 \pm 201.1\ mW/m^2$) was 26.8–62.3% higher than those in stage 1, 2, and 4. These average power densities were comparable to that obtained in a three-chamber MDC system (from 776 ± 30 to $931 \pm 29\ mW/m^2$) with released pH imbalance in electrode chambers by operating the reactors in an internal recirculation mode [24].

The final pHs were 4.43 ± 0.17, 6.18 ± 0.16, 5.95 ± 0.08, 5.95 ± 0.02 for the anolytes, and 10.72 ± 0.03, 10.65 ± 0.08, 10.56 ± 0.07, 10.55 ± 0.04 for the catholytes in four stages respectively (Fig. 3). The lower HRT for anode chamber (24 h, stage-1; 12 h, stage 2–4) prevented sharp decrease in anolyte pH, however, the pH of catholyte approached almost same regardless of the different HRTs for cathode chamber. This pH results also suggested that cathode pH is not as critical as anode pH to reactor performance. Inhibition of exoelectrogenic activity resulting from low pH of anolyte accounted for the low power generation during MDC operation. The COD removal rates for MDCs were $1.84 \pm 0.05\ kgCOD/(m^3\ d)$ in stage 3, higher than those observed in other three stages ($0.87 \pm 0.04\ kgCOD/(m^3\ d)$, stage 1; $1.70 \pm 0.06\ kgCOD/(m^3\ d)$, stage 2; $1.47 \pm 0.04\ kgCOD/(m^3\ d)$, stage 4). The first MDC (MDC-1) of the four MDCs operated in series had the best performance in substrate degradation, compared to the other three MDCs downstream ($1.80 \pm 0.14\ kgCOD/(m^3\ d)$, stage 1; $2.98 \pm 0.25\ kgCOD/(m^3\ d)$, stage 2; $3.42 \pm 0.22\ kgCOD/(m^3\ d)$, stage 3; $2.77 \pm 0.21\ kgCOD/(m^3\ d)$, stage 4) (Fig. S2). There were two main factors resulting in the relatively lower COD removal rates of downstream MDCs: (1) inchoate pH inhibition in anode chamber and (2) transport of chloride ions into anode chamber increased osmotic pressure, which deactivated exoelectrogens in downstream MDCs [25]. Also, dissolved oxygen was not removed from the influent and this could have resulted in aerobic oxidation of substrate by aerobic microorganisms in MDC-1 compared to downstream MDCs.

The overall CEs varied with different HRTs ($26.4 \pm 2.5\%$, stage 1; $15.7 \pm 1.5\%$, stage 2; $19.4 \pm 1.6\%$, stage 3; $11.7 \pm 1.1\%$, stage 4) (Fig. S2). The CEs of second MDC were relatively higher than the first MDC, and then the CEs further decreased in the third and fourth MDCs. The lower CEs for the first MDCs were due to loss of substrate via aerobic oxidation when there was oxygen dissolved in the influent. The CEs decreased in the second through the fourth MDCs, mainly due to reduced current production in the direction of flow resulted from substrates consumption and limited mass transfer in anode and cathode chamber.

3.2. The desalination performance of MDCs

The desalination performance showed similar tendency as current generation in different stages. The reactors in particular stage with higher current generation also possessed better removal of salt than other stages (Fig. 4). The four MDCs in stage 1 and stage 2 produced average current of 21.7 ± 8.2 mA and 26.1 ± 4.1 mA, with the overall removals for salt was $50.9 \pm 3.5\%$ and $55.9 \pm 2.9\%$ respectively. With an average current increase to 27.5 ± 3.6 mA in stage 3, the salt removal increased to $76.5 \pm 1.2\%$. However, a slight decrease of 7.7% in average current from 26.1 ± 4.1 mA in stage 2–24.1 ± 3.7 mA in stage 4, led to a higher salt removal of $68.8 \pm 1.6\%$. This might be salt permeation without the effect of being driven by electric field under higher concentration difference between desalination chamber and concentrated chamber because of the increased flowrate of tap water in the concentrated chamber in stage 4. Besides, it could also be attributed to waster osmosis between desalination chamber and concentrated chamber [26]. This phenomenon of salt permeation without current generation was also observed in a previous study where the ion mobility occurred under open circuit condition [27]. The total rates of desalination in the four stages were 35.7 ± 2.5, 39.1 ± 2.1, 53.6 ± 0.8, $48.2 \pm 1.1\ kg/(m^3\ d)$, which was much greater than previously obtained in a milliliter-sized MDCs operated in series ($5.21 \pm 0.05\ kg/(m^3\ d)$) [28]. A similar decrease in salinity removal performance along the length of flow was observed on the basis of just the analysis of a single stage, attributing to the gradual decline of current generation from MDC-1 to MDC-4. The salt ions migrated from desalination chamber to concentrate chamber producing the salt concentrations in the concentrate effluent of 9.8 ± 0.8, 8.9 ± 0.6, 6.8 ± 0.1, 3.1 ± 0.3 g/L in stage 1–4 respectively, which was enough for conductivity requirement of cathode reaction.

It was worth noting that the two desalination chambers showed a slight difference in desalination performance. The desalination chamber near cathode showed better salt removal rates than that near anode. The reason for the discrepant desalination performance

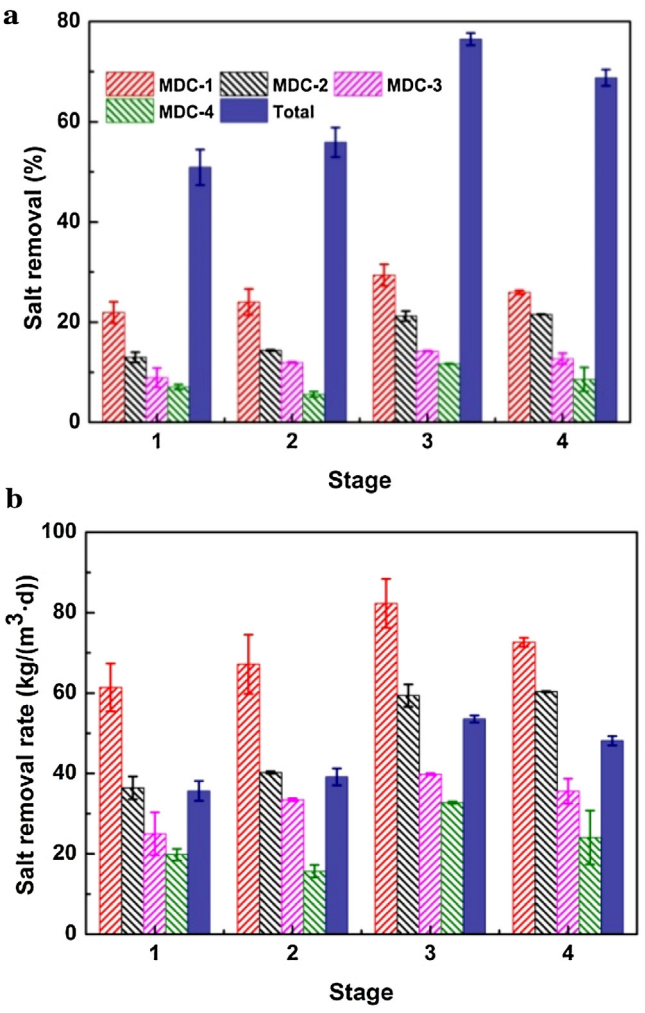

Fig. 4. Desalination performance of the series of hydraulically connected MDCs in four stages. The salt removal was based on the average of the second and fourth chambers.

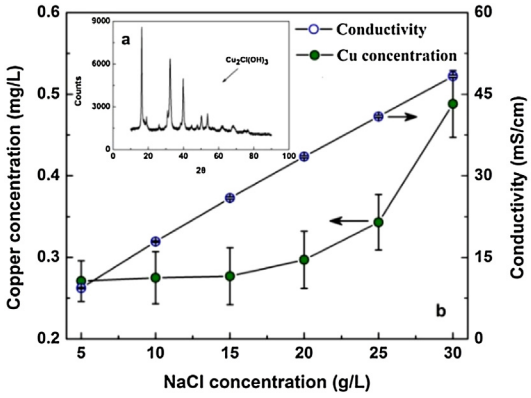

Fig. 5. X-ray diffraction pattern of the precipitate in the sedimentation tank (a) and salt effect on copper removal at neutral pH (b).

could be the volume difference between anode chamber and cathode chamber. The amount of solution used in the anode chamber was much larger than that of cathode chamber (10:1), and the anolyte flowrate was 16.7 times higher than that of catholyte. With a low volume ratio of desalination chamber to anode chamber, the anode chamber acted as huge high-salinity-water pool with a high concentration of phosphate in the buffer solution migrating to desalination chamber through the AEM, which decreased the salt removal of the desalination chamber near anode.

3.3. Heavy metal removal

A high catholyte pH was essential for copper removal. The catholyte effluents were all maintained at around pH of 10.6, in spite of the difference in operational conditions in four stages. The 4-MDCs system operating under stage 3 was the best choice functioning as "alkalinity donor" for post-precipitation treatment, considering its higher electricity production.

For practical application, it is important to keep durable and stable removal performance for providing effluent quality assurance. Various concentrations of copper-containing wastewaters (800, 1000, 1500, 5000 mg/L) were used as influent to simulate a fluctuation in discharge strengths in the case of unstable washing water dosage. The pH of these copper-containing wastewaters was all fixed initially at pH = 3 to simulate real wastewaters with high acidity, and the effluents were controlled at neutral pH. Theoretically, the concentration of Cu^{2+} starts to reduce at pH 5.12, 5.07, 4.99, and 4.72 under initial concentrations of 800 mg/L, 1000 mg/L, 1500 mg/L, and 5000 mg/L ($K_{sp} = 2.2 \times 10^{-20}$). To meet the emission standard for electroplating of China (0.5 mg/L, GB 21900-2008), the final pH needs to be controlled above 6.72. In this study, copper precipitated near the theoretical pH level, and a blue precipitate was observed at the bottom of the reactor with obvious solid-liquid boundary. XRD studies of the precipitate indicated the presence of $Cu_2Cl(OH)_3$ (Fig. 5a). This formation of $Cu_2Cl(OH)_3$ might be attributed to the Cl^--rich environment, which was also reported by other researchers [29]. There was nearly complete removal of copper under various initial copper concentrations. A maximum copper removal rate of 5.07 kg/(m^3 d) (based on cathode volume of MDC) was obtained under the influent concentration of 5000 mg/L, with the emission concentration of 0.27 ± 0.03 mg/L.

A potential concern with using the high-conductivity catholyte effluent of MDC as "alkalinity donor" for copper removal was the higher residual copper concentration after precipitation compared to theoretical value. This difference between experimental and theoretical values was correlated to salt effect stimulated by high NaCl concentration in the catholyte effluent. To further confirm the salt effect on residual copper concentration, tests with 5 mg $CuCl_2$ powder added into six different concentration gradients of NaCl solution (5, 10, 15, 20, 25, 30 g/L, volume of 1 L) were conducted. The residual copper concentrations at neutral pH were compared under various salinities. A slight increase of copper concentration in supernatant from 0.271 ± 0.025 mg/L to 0.297 ± 0.035 mg/L was observed with the salt concentration increment from 5 g/L to 20 g/L. Further increment in salt concentration to 25 g/L resulted in a higher copper concentration of 0.343 ± 0.034 mg/L. When the salt concentration was 30 g/L, the copper concentration increased to 0.488 ± 0.041 mg/L (Fig. 5b). This result demonstrated that salinity played an important role in effluent quality, and treatment efficiency could be only assured in certain salinity domain.

3.4. The performance of MDC-powered ED system

The capacitor-based circuit was applied to increase the discharging voltage to meet voltage requirement for ED system by means of the adjustment of switching time (T_s). The set-1 of MDC-1 and MDC-2 possessed better electricity generation capability than set-2 of MDC-3 and MDC-4 in terms of charging potential (V_c) and discharging voltage (V_d) (Fig. 6). The charging and discharging voltage of set-1 at T_s of 15 min varied in range from 174 ± 7 mV to 426 ± 4 mV, while the corresponding value of set-2 ranging from 154 ± 6 mV to 371 ± 5 mV. This difference of charging and discharg-

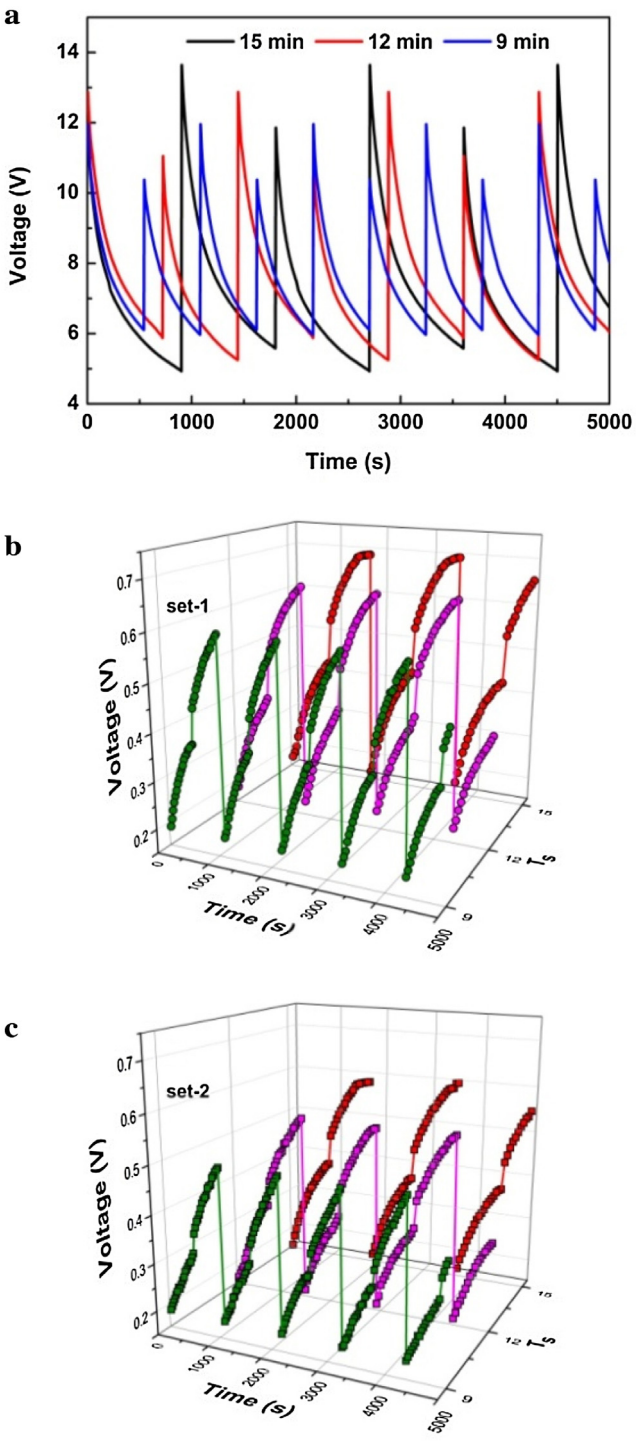

Fig. 6. The discharging voltage of the capacitor-based circuit (a) and change of voltage across the set-1 and set-2 (b–c) at different T_s.

ing voltage between two sets was equivalent to the additional power output of 4.42 mW. A remarkable difference of power output between the two sets was also observed at T_s of 12 min (5.23 mW) and 9 min (6.43 mW). Besides, the charging and discharging voltage of each set appeared to be more differentiated with the increase of T_s.

The curves showed that the maximum discharging voltage came out higher while the minimum discharging voltage was lower with the increase of T_s. The maximum discharging voltages (12.75 ± 1.26 V) was obtained for T_s of 15 min, followed by 12 min

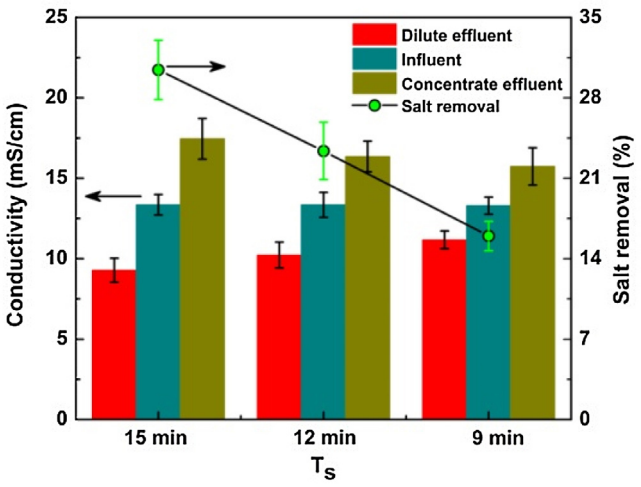

Fig. 7. The desalination performance of the ED system powered by MDCs.

(11.96 ± 1.29 V) and 9 min (11.17 ± 1.11 V). The corresponding minimum discharging voltages were 5.26 ± 0.46 V, 5.57 ± 0.45 V and 6.04 ± 0.10 V, respectively. The average discharging current gradually increased with the decrease of T_s. The current obtain when operating at T_s of 9 min was 7.0% and 14.1% higher than those when operating at T_s of 12 min and 15 min. This change of discharging voltage and current consisted of an initial rapid decrease and a following gradual decrease, indicating a non-uniform desalination rate in a charging and discharging cycle. Performance at shorter T_s also produced a higher average discharging power than the longer T_s (15.54 ± 2.21 mW, 15 min; 16.16 ± 2.61 mW, 12 min; 16.98 ± 3.21 mW, 9 min).

As the ions in the desalination chamber continuously migrated to concentrated chamber, the dilute conductivity presented a decline and that of concentrate had an increase (Fig. 7). The desalination efficiency of ED system at T_s of 15 min achieved 30.4 ± 2.6%, with final conductivity of the dilute reducing to 9.28 ± 0.75 mS/cm while concentrate increasing to 17.45 ± 1.27 mS/cm. With T_s decreasing to 12 min, the dilute conductivity decreased to 10.23 ± 0.79 mS/cm with desalination efficiency of 23.4 ± 2.5%, while the concentrate conductivity increased by 22.5% to 16.35 ± 0.95 mS/cm. A further decrease in T_s to 9 min, the desalination efficiency slightly dropped to 15.9 ± 1.3% (dilute conductivity of 11.17 ± 0.55 mS/cm). The concentration of residual copper after precipitation treatment also presented a decline (0.15 ± 0.03 mg/L, T_s = 15 min; 0.18 ± 0.02 mg/L, T_s = 12 min; 0.21 ± 0.03 mg/L, T_s = 9 min) in the dilute effluents. It was worth noting that the change tendency of desalination efficiency presented an inverse correlation with average discharging power when T_s decreased from 15 min to 9 min. This meant the electricity that could be used as "qualified" driving force for ion mobility was limited in a certain range, considering the voltage attenuation in the discharging process (detailed analysis with a comparative study using DC power supply in the SI). Though the desalination performance needed to be further improved, such unique system utilizing the electricity produced by MDCs for salt removal using ED still offered three benefits: (1) electrical energy produced by MDCs could be used effectively instead of dissipating as heat through resistor; (2) converting salt water into useable reclaimed water to extend water supplies; (3) further elimination of trace copper after precipitation treatment.

Compared to continuous energy harvesting using the resistance, the capacitor-based circuit significantly increased the energy output of MDCs. At T_s varying from 15 min to 9 min, the average discharging power was 40.5-53.5% higher than those when

MDCs were connected with resistance at maximum power point (11.06 ± 3.01 mW). The capacitor-based circuit allowed MDCs to harvest electrical energy of 4.14 ± 0.59 kWh, 4.31 ± 0.71 kWh, 4.53 ± 0.86 kWh (normalizing to 1 m^3 of salt solution treated). This energy recovery mode using capacitor producing more energy than conventional continuous energy harvesting using resistance, has also been reported in previous studies [30]. From an engineering point of view, it was of great meaning to offset the energy requirement for ED system using the energy recovery from MDCs. For example, to desalinate the salt solution to <20 μS/cm which was comparable to drinking water in terms of salinity, the MDCs could provide 2.9–3.2% of electrical energy needed (according to the comparative study using DC power supply in SI, Fig. S3 and S4). In an industrial process, this 2.9–3.2% of electrical energy consumption is equivalent to huge economic cost, which helps to address energy shortage.

3.5. Perspectives

This combined system was attractive because the MDC was no longer a passive desalination device, but also an "alkalinity donor" and "real power supply". Three separate innovations were used to spread its applied fields. (1) A novel water flow scheme through the stack. The use of concentrate as catholyte influent provided two potential benefits: minimizing amount of influent lines and decreasing the complexity of the water distribution system. (2) The elimination of need for a pH-controlled catholyte. The alkalinity produced by cathode reaction was desirable for copper removal in this study, which refused the use of buffered catholyte. (3) MDC-powered ED system for a deep desalination. Although the desalination performance remained to be improved compared to DC power supply, it still provide us a new enlightenment for deep salt removal through in-situ utilization of generated electricity. Nevertheless, several challenges still remain to be overcome for real-world application, for instance, the introduction of multiple metals in the wastewater and configuration optimization of ED reactor. With these further studies, it should be possible to better evaluate the feasibility of the combined system for real-world application.

4. Conclusion

A 4-MDCs system was successfully utilized to produce alkalinity for copper-containing wastewater treatment and simultaneously salt removal. By adjusting the operation conditions of MDC, the best performance in terms of power generation, salt removal, and COD removal rate was achieved in stage 3. There was nearly complete removal of copper, with the emission concentration (0.27 ± 0.03 mg/L) meeting the emission standard for electroplating of China (0.5 mg/L, GB 21900-2008) Moreover, the salt effluent after sedimentation was subjected to deep desalination by an ED system powered by MDCs. Energy analysis demonstrated that MDCs could provide 2.9–3.2% of total electrical energy needed for the ED system to produce high quality effluent with conductivity <20 μS/cm. Overall, these results suggested a promising application for heavy metal removal and simultaneous deep desalination of high-salinity-water after further study.

Acknowledgements

This work was supported by the National Natural Science Fund for Distinguished Young Scholars (Grant No. 51125033), National Natural Science Fund of China (Grant No. 51209061), National Natural Science Fund of China (51209061 and 51308171) funded by China Postdoctoral Science Foundation (2016M591534) and the Fundamental Research Funds for the Central Universities (HIT. NSRIF. 2015090). The authors also acknowledged the International Cooperating Project between China and European Union (Grant no. 2014DFE90110).

Appendix A. Supplementary data

Supplementary data associated with this article can be found, in the online version, at http://dx.doi.org/10.1016/j.jhazmat.2016.08.034.

References

[1] W.-W. Li, H.-Q. Yu, Z. He, Towards sustainable wastewater treatment by using microbial fuel cells-centered technologies, Energy Environ. Sci. 7 (2014) 911–924.
[2] M.T. Myint, A. Ghassemi, N. Nirmalakhandan, Complete sustainability in electrodialysis reversal desalination: reusing tertiary-treated municipal wastewater as feed in the concentrate stream and electrodes rinsing water, Desalin. Water Treat. 51 (2013) 3215–3223.
[3] J. Liu, X.H. Zhang, H. Tran, D.Q. Wang, Y.N. Zhu, Heavy metal contamination and risk assessment in water paddy soil, and rice around an electroplating plant, Environ. Sci. Pollut. R 18 (2011) 1623–1632.
[4] U.N., UN, International decade for action 'Water for life', Water Scarcity, 2005–2015.
[5] Z. Ge, L. Wu, F. Zhang, Z. He, Energy extraction from a large-scale microbial fuel cell system treating municipal wastewater, J. Power Sources 297 (2015) 260–264.
[6] F. Fu, Q. Wang, Removal of heavy metal ions from wastewaters: a review, J. Environ. Manag. 92 (2011) 407–418.
[7] D. Mani, C. Kumar, Biotechnological advances in bioremediation of heavy metals contaminated ecosystems: an overview with special reference to phytoremediation, Int. J. Environ. Sci. Technol. 11 (2013) 843–872.
[8] J.L. Huisman, G. Schouten, C. Schultz, Biologically produced sulphide for purification of process streams, effluent treatment and recovery of metals in the metal and mining industry, Hydrometallurgy 83 (2006) 106–113.
[9] R. Baciocchi, G. Storti, M. Mazzotti, Process design and energy requirements for the capture of carbon dioxide from air, Chem. Eng. Proc. 45 (2006) 1047–1058.
[10] M. Mahmoudkhani, D.W. Keith, Low-energy sodium hydroxide recovery for CO2 capture from atmospheric air—thermodynamic analysis, Int. J. Greenh. Gas Control 3 (2009) 376–384.
[11] T. Richards, C. Pavletic, J. Pettersson, Efficiencies of NaOH production methods in a Kraft pulp mill, Int. J. Energy Res. 33 (2009) 1341–1351.
[12] A.H. Galama, M. Saakes, H. Bruning, H.H.M. Rijnaarts, J.W. Post, Seawater predesalination with electrodialysis, Desalination 342 (2014) 61–69.
[13] Y. Kim, B.E. Logan, Microbial desalination cells for energy production and desalination, Desalination 308 (2013) 122–130.
[14] B. Zhang, Z. He, Energy production, use and saving in a bioelectrochemical desalination system, RSC Adv. 2 (2012) 10673–10679.
[15] H. Luo, P.E. Jenkins, Z. Ren, Concurrent desalination and hydrogen generation using microbial electrolysis and desalination cells, Environ. Sci. Technol. 45 (2011) 340–344.
[16] X. Chen, X. Xia, P. Liang, X. Cao, H. Sun, X. Huang, Stacked microbial desalination cells to enhance water desalination efficiency, Environ. Sci. Technol. 45 (2011) 2465–2470.
[17] Y. Kim, B.E. Logan, Series assembly of microbial desalination cells containing stacked electrodialysis cells for partial or complete seawater desalination, Environ. Sci. Technol. 45 (2011) 5840–5845.
[18] R.A. Rozendal, H.V.M. Hamelers, K. Rabaey, J. Keller, C.J.N. Buisman, Towards practical implementation of bioelectrochemical wastewater treatment, Trends Biotechnol. 26 (2008) 450–459.
[19] F. Zhang, K.S. Jacobson, P. Torres, Z. He, Effects of anolyte recirculation rates and catholytes on electricity generation in a litre-scale upflow microbial fuel cell, Energy Environ. Sci. 3 (2010) 1347.
[20] H. Dong, H. Yu, X. Wang, Q. Zhou, J. Feng, A novel structure of scalable air-cathode without Nafion and Pt by rolling activated carbon and PTFE as catalyst layer in microbial fuel cells, Water Res. 46 (2012) 5777–5787.
[21] D. Pant, G. Van Bogaert, L. Diels, K. Vanbroekhoven, A review of the substrates used in microbial fuel cells (MFCs) for sustainable energy production, Bioresour. Technol. 101 (2010) 1533–1543.
[22] A.T. Heijne, F. Liu, R. van der Weijden, J. Weijma, C.J.N. Buisman, Copper recovery combined with electricity production in a microbial fuel cell, Environ. Sci. Technol. 44 (2010) 4376–4381.
[23] Y. Dong, Y. Feng, Y. Qu, Y. Du, X. Zhou, J. Liu, A combined system of microbial fuel cell and intermittently aerated biological filter for energy self-sufficient wastewater treatment, Sci. Rep. 5 (2015) 18070.
[24] Y. Qu, Y. Feng, J. Liu, W. He, X. Shi, Q. Yang, J. Lv, B.E. Logan, Salt removal using multiple microbial desalination cells under continuous flow conditions, Desalination 317 (2013) 17–22.

[25] Z. An, H. Zhang, Q. Wen, Z. Chen, M. Du, Desalination combined with copper(II) removal in a novel microbial desalination cell, Desalination 346 (2014) 115–121.
[26] Q. Ping, B. Cohen, C. Dosoretz, Z. He, Long-term investigation of fouling of cation and anion exchange membranes in microbial desalination cells, Desalination 325 (2013) 48–55.
[27] K. Zuo, J. Cai, S. Liang, S. Wu, C. Zhang, P. Liang, X. Huang, A ten liter stacked microbial desalination cell packed with mixed ion-exchange resins for secondary effluent desalination, Environ. Sci. Technol. 48 (2014) 9917–9924.
[28] Y. Qu, Y. Feng, X. Wang, J. Liu, J. Lv, W. He, B.E. Logan, Simultaneous water desalination and electricity generation in a microbial desalination cell with electrolyte recirculation for pH control, Bioresour. Technol. 106 (2012) 89–94.
[29] H.-C. Tao, M. Liang, W. Li, L.-J. Zhang, J.-R. Ni, W.-M. Wu, Removal of copper from aqueous solution by electrodeposition in cathode chamber of microbial fuel cell, J. Hazard. Mater. 189 (2011) 186–192.
[30] P. Liang, W. Wu, J. Wei, L. Yuan, X. Xia, X. Huang, Alternate charging and discharging of capacitor to enhance the electron production of bioelectrochemical systems, Environ. Sci. Technol. 45 (2011) 6647–6653.